Polymers Tethered to Curved Interfaces. A Self-Consistent-Field Analysis

N. Dan and M. Tirrell*

Department of Chemical Engineering and Material Science, University of Minnesota, Minneapolis, Minnesota 55455

Received November 4, 1991; Revised Manuscript Received February 15, 1992

ABSTRACT: We consider the equilibrium properties of chains tethered by one end to a curved, impenetrable interface, using a self-consistent-field model. The segment density profiles, layer thickness, and distribution of chain ends are numerically calculated. The interface curvature at which chain properties significantly deviate from the planar limit is, as anticipated, of the same order of magnitude as the chain dimensions. The chain dimensions follow scaling power laws only in the limit of high interface curvature or chain molecular weight. An exclusion zone in the distribution of chain ends appears near the interface, the size of which depends linearly on layer thickness. The ratio of exclusion zone height to brush thickness does not decrease smoothly with interface curvature but obtains maximum values at finite interface radii. The corrections to the value of the ratio of exclusion zone height to brush thickness, in the limit of infinite molecular weight, scale reasonably well with an anticipated molecular weight power law of $-1/3$.

Introduction

The study of chains tethered to one end to a curved interface under good solvent conditions influences such diverse systems as chains grafted on small colloidal particles, the corona of polymer micelles, or the arms of star and comb polymers. The properties of end-constrained polymer chains strongly differ, at high tether densities, from those of free chains. Tethering forces the chains to deform from the free-chain, random-walk isotropic configuration, causing them to stretch in the direction perpendicular to the interface, thus forming a brushlike structure.[1,2]

Accounting for interface curvature effects is crucial in the discussion of brushes on highly curved interfaces. This is due to the fact that the volume accessible to the chains increases as a function of the distance from the tether site. Local stretching therefore diminishes with the distance from the surface, so that the chains are globally less stretched than similar structures on planar interfaces. Several approaches have been used to model these systems, including molecular dynamics simulations (MD)[3,4] and self-consistent-field (SCF)[5] and scaling theories.[6,7]

Scaling models make use of simple free energy balance arguments while accounting for correlations in the chain configurations. All chain ends are assumed to be at the same height above the interface (see Figure 1). The entropic tendency of the chains to adopt a contracted, random-walk configuration is balanced with the solvent–monomer interactions, which favor a swollen configuration. The original scaling model developed by Alexander[8] and de Gennes[9] for chains on planar interfaces has been later extended to curved interfaces through simple geometrical considerations.[6,7] The segment density profile decreases with the radius as

$$\phi(r) \sim \sigma^{2/3}(R/r)^{2D/3} \tag{1}$$

where ϕ is the segment density distribution, σ is the dimensionless surface density, and R is the interface radius of curvature. D is related to the dimensionality of curvature in the geometry under consideration and is equal to 0 in planar geometry, 1 for cylinders, and 2 for spheres. The average brush height $\langle L \rangle$ can be calculated from the segment density profile and is approximately given by

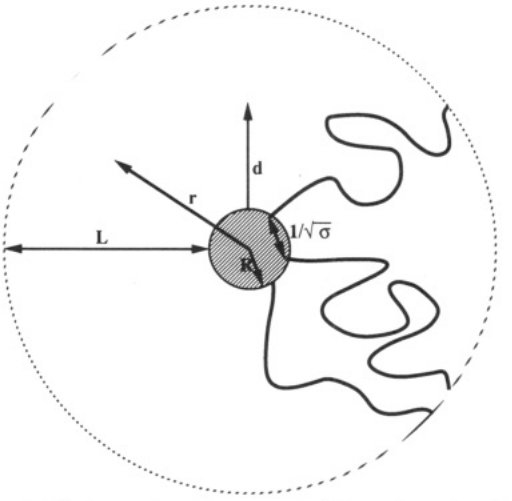

Figure 1. Chains tethered on a curved interface of radius R. r denotes the radial distance and d the height from the interface. L is the brush thickness.

$$\langle L \rangle \sim aN^{3/(3+D)}\sigma^{1/(3+D)}(R/a)^{D/(3+D)} \tag{2}$$

The scaling predictions have been examined, and to some extent confirmed, by molecular dynamics simulations of star polymers[3] and of chains grafted on a cylindrical interface[4] under good solvent conditions. Chain dimensions were found to be in good agreement with the predictions of eq 2. The segment density profile, in both geometries, showed a peak near the interface (or star core) followed by a region of power law decay as a function of the radius. In the case of star polymers, a slope of 1.25, approaching the scaling prediction (eq 1) of $\phi \sim r^{-4/3}$, was observed. However, for chains on cylindrical interfaces, the density profile decreased with the square root of the radius and not as the expected $-2/3$ power law.[7]

Scaling models impose strong restrictions on the chain conformations, namely, that all chain ends are located at the same height and fluctuations in chain extension are ignored. Therefore, they cannot provide insights into the internal structure of the polymer layer. Relaxation of these constraints leads to the self-consistent-field theory, where

0024-9297/92/2225-2890$03.00/0 © 1992 American Chemical Society

neither the segment density profile nor the distribution of chain ends is predetermined. The chain configurations are obtained by solving a diffusion-type equation subject to a pressure potential,[10] which in turn depends on the chain configurations. The pressure potential defines the work required to stretch the chains in order to accommodate a test segment at a given height. It was first noted by Semenov[11] that the dominant configuration of a strongly stretched chain, as is the case in a densely grafted brush, is reminescent of the trajectory of a classical particle. This analogy enabled Milner et al.[12] to obtain an analytical solution for chains tethered on a planar interface. The authors assumed that the chain ends could be located at any height throughout the brush, since chains with free ends near the surface reduce their stretching energy but have increased segment–segment repulsion, and vice versa for chains with free ends far from the interface. The segment density profile and pressure potential fied were found to be parabolic, of the form $A-Bz^2$, where z is the height from the interface.

In an extension of this approach, Ball et al.[5] considered the equilibrium properties of chains tethered to convex interfaces. It was shown that, as the curvature increases, a zone from which chain ends are excluded should appear next to the interface. The chain ends are in effect expelled from the vicinity of the interface by the sharp segment density gradient. The case of brushes grafted on cylindrical interfaces in the melt state, where no solvent penetrates into the brush, was solved analytically. Unlike the case of a swollen brush, where the segment density is proportional to the potential field profile, the melt brush segment density is uniform. The potential field acting on the chains, though, is not. Unlike the parabolic profile of the planar brush, the pressure profile was found to be concave up throughout the layer, in the limit of high interface curvature. The height of the exclusion zone, in that limit, approached the value of $(2/\pi)\langle L\rangle$, decreasing smoothly with interface curvature. Although the equations describing spherical interfaces and brushes in a good solvent were not solved, the authors estimated that a significant exclusion zone would exist under those conditions as well.

This analysis[5] applies to chains in the limit of high molecular weight and low surface density. It should be noted that MD simulations of chains grafted on cylindrical interfaces[4] under good solvent conditions did not show a chain end exclusion zone near the interface for finite interface radii. A narrow exclusion zone appeared only in a limit case of densely grafted chains on a line ($R/a \sim 0$). The authors[4] attributed this exclusion zone to simple steric packing constraints, since the high grafting density prevented penetration of the free end of the chains to the region near the interface.

In this paper, we apply the Dolan–Edwards[10] SCF equation to systems of chains in a good solvent, densely tethered to curved interfaces, both spherical and cylindrical. We investigate the equilibrium properties of these systems at various interface curvatures, chain molecular weights, and grafting densities. Our aim is to determine whether scaling model predictions for the segment density and layer thickness apply, and what is the characteristic curvature where brush properties start to deviate from those of the planar brush. We also investigate under what conditions the Ball et al.[5] analytical solution holds, especially regarding the conditions leading to the appearance of a chain end exclusion zone. The self-consistent-field model allows us to investigate high molecular-weight, high surface density systems which cannot be obtained by MD simulations due to computing time limitations. This enables us to approach the high molecular weight limit more closely and investigate asymptotic analytical model predictions more extensively than by simulations. The presence and properties of an exclusion zone in the chain end distribution are significant, since they can be manipulated to localize the chain ends at the outer perimeter of the brush, thereby enabling tailoring of the segment distribution near the brush surface.

The Self-Consistent-Field Model

The configurations of a polymer segment in a system with excluded-volume interactions are a function of the position of all other segments in the system. In SCF models, this effect is incorporated not by excluding segments from occupied positions but through a potential field creaeted by the configurations of all other segments. The potential field, in turn, is a function of the segment distribution, hence, the self-consistency. Chain statistics can therefore be described as those of a random walk under an average potential field. In dilute and semidilute systems, the potential is reasonably taken to be proportional to the local segment density (ϕ).[10]

We consider monodisperse polymer chains with N segments of a length each, tethered at a density of σ/a^2 chains per unit area to an interface. The distribution function $Q(\mathbf{r},\mathbf{r}';n)$ denotes the statistical weight of a subchain starting at a spatial position $\mathbf{r}'$ and ending at a position $\mathbf{r}$ in n steps, without crossing a confining surface. The distribution function satisfies the partial differential equation

$$\frac{\partial Q}{\partial n} = \frac{a^2}{6}\nabla^2 Q - \upsilon\phi(\mathbf{r})Q(\mathbf{r},\mathbf{r}';n) \tag{3}$$

where υ is the excluded-volume parameter. The initial condition is given by $Q(\mathbf{r},\mathbf{r}';0) = \delta(\mathbf{r}-\mathbf{r}')$, and the boundary condition on the confining surface is $Q(\mathbf{r},\mathbf{r}';n) = 0$.

At relatively high surface density, Q can be assumed to vary as a function of the direction perpendicular to the interface only. Therefore, in spherical and cylindrical geometries, $\mathbf{Q}$ depends on the segment number n and the radius r. ϕ is taken to be the average local segment density.

The average local segment density can be calculated by summing the probability of configurations passing through a spatial point:

$$\phi(r) = \psi\frac{\int_0^N \mathrm{d}n \int_R^\infty \mathrm{d}V'\, Q(R,r;n)\, Q(r,r';N-n)}{\int_R^\infty Q(R,r';N)\, \mathrm{d}V'} \tag{4}$$

$\mathrm{d}V'$ is $r^2\,\mathrm{d}r$ in spherical coordinates and $Lr\,\mathrm{d}r$ in cylindrical ones, where L is the cylinder length. ψ is a normalization factor and can be calculated using the stipulation that the total number of segments in the system is equal to the sum of all segments in the segment density distribution.

Solving the partial differential equation (eq 3) under the constraint of eq 4 for the average local density produces the self-consistent profile. We use a numerical procedure similar to that of Dolan and Edwards,[10] where space is discretized into steps of length a, the segment size. The volume element $\mathrm{d}V$ is, therefore, equal to the volume of a radial shell of thickness a. An initial guess is taken for the distribution function, or, in our case, the ideal random-walk distribution function. Using this function, the local segment density is calculated and inserted into the partial differential equation, leading to calculation of a new distribution function. Iterations were stopped when the relative difference between new and previous iteration

segment distributions was less than 10^{-8}. In all calculations, the excluded-volume parameter v is set to unity, stipulating a good solvent environment.

Once the distribution function and the local segment density are obtained, system properties can be evaluated. The brush thickness is usually calculated from the second moment of the segment density distribution:

$$\langle L \rangle = \left\{ \frac{\int_R^\infty dV' \, r'^2 \, \phi(r')}{\int_R^\infty dV' \, \phi(r')} \right\}^{1/2} - R \qquad (5a)$$

However, when the radius of the interface increases, dV' and r' become increasingly large numbers. Integration then magnifies small round-off errors in the calculated profile. We find that a more accurate measure of the brush thickness, especially in the limit of low interface curvatures, is obtained by averaging the height d ($=r - R$):

$$\langle L \rangle = \left\{ \frac{\int_R^\infty dV' \, d^2 \phi(r')}{\int_R^\infty dV' \, \phi(r')} \right\}^{1/2} \qquad (5b)$$

We therefore use this height average to define the brush thickness. All length scales in the system are given in units of a, the segment size.

The normalized distribution of chain ends can be calculated from the probability distribution. It is proportional to the probability that a chain starting at R, the interface, will reach a position r in N steps:

$$\epsilon(r) = \frac{dV \, Q(R,r;N)}{\int_R^\infty dV' \, Q(R,r';N)} \qquad (6)$$

Results

In order to enable comparison with scaling models[6-9] and SCF analytical solutions,[5,12] which apply to stretched chains, we limit our calculations to comparatively dense, high molecular weight systems. In the test case chosen of $N = 100$ and $\sigma = 0.1$, tethered on surfaces of radius $R = 10$, the brush thickness, $\langle L \rangle$, is calculated from eq 5b to be 21.1 for cylindrical and 18.3 for spherical interfaces. The average thickness of an isolated ($\sigma \sim 0$) tethered chain of this length is 10.8. Therefore, in both geometries the stretching ratio is approximately 2 and will increase with either N or surface density. In comparison, an identical layer on a planar interface (L_0) has a layer thickness of 24.4.

The effect of interface curvature on the segment density distribution, for chains of $N = 100$, is shown in Figure 2. The distribution of chains tethered on the low-curvature interfaces ($R = 100$) approaches the parabolic limit of the planar interface.[12,13,19] The segment density distribution, which is proportional to the potential, resembles in the limit of high interface curvature the pressure profile of brushes in the melt.[5] Note that the case of $R = 1$ in Figure 2a is that of a star polymer,[14] whereas the profile of $R = 1$ in Figure 2b represents that of the arms of a polymacromonomer with a locally straight backbone.[15] The segment density profiles as a function of N and σ are shown in Figure 3, for chains tethered on spherical and cylindrical interfaces of radius 10. The segment density distribution shows a peak near the interface, the position of which is insensitive to either chain molecular weight or surface density. Peak height is independent of chain molecular weight, as in the case of chains tethered on planar interfaces.[13,19] Figure 4 shows that the segment density profiles scale in both geometries with $\sigma^{2/3}$ and are

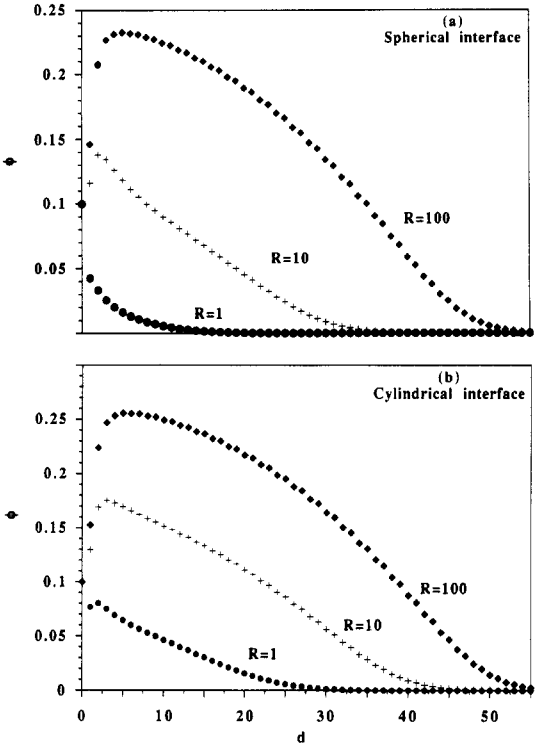

Figure 2. Segment density distribution for $N = 100$ and $\sigma = 0.1$ chains tethered on curved interfaces: (a) Spherical geometry. (b) Cylindrical geometry. (◆) $R/a = 100$, (+) $R/a = 10$, (●) $R/a = 1$.

insensitive to chain molecular weight in the power law region, as predicted by scaling models in eq 1. The falloff of segment density with radius for chains tethered on spherical interfaces seems to be approaching, from below, the scaling prediction of an $r^{-4/3}$ power law in the interior of the brush. This is in agreement with the observation of a 1.25 power law in MD simulations[4] of dense stars. In the case of cylindrical interfaces, the power law exponent has an approximate value of $-1/2$ and not the expected $-2/3$ of eq 1. A similar value was found for the power law decay region in the MD simulations[3] of chains tethered on a line ($R = 1$).

The brush thickness as a function of chain molecular weight clearly reaches the asymptotic limit predicted by eq 2 at high interface curvature and chain molecular weight, as seen in Figure 5. This is another example[1,2] of the ability of scaling models to predict global brush features well, even when inaccurately describing the segment density profile. As interface curvature decreases, the layer thickness increases toward the planar brush $\langle L_0 \rangle \sim N^{1.0}$. In order to determine the characteristic interface radius at which brush structure starts to deviate from the planar limit, we examine the dependence of brush thickness on the interface radius. Figure 6 shows significant deviations from the planar interface layer thickness, $\langle L_0 \rangle$, developing at values of R/L_0 smaller than 10. The characteristic ratio where deviations start to appear is insensitive to variations in surface density or chain molecular weight and seems to be independent of interface geometry. This result is somewhat surprising since chains on a cylindrical interface are more stretched than their spherically tethered counterparts and should therefore be closer in structure to the planar brush.

The distribution of the chain ends as a function of the interface radius is shown in Figure 7. In the case of dense stars, the distribution of the chain ends has been shown to approach a Gaussian shape.[18] In comparison, in the planar brush[12,19] $\epsilon(d) \sim (d/\langle L \rangle)\{1 - (d/\langle L \rangle)^2\}^{1/2}$. From a

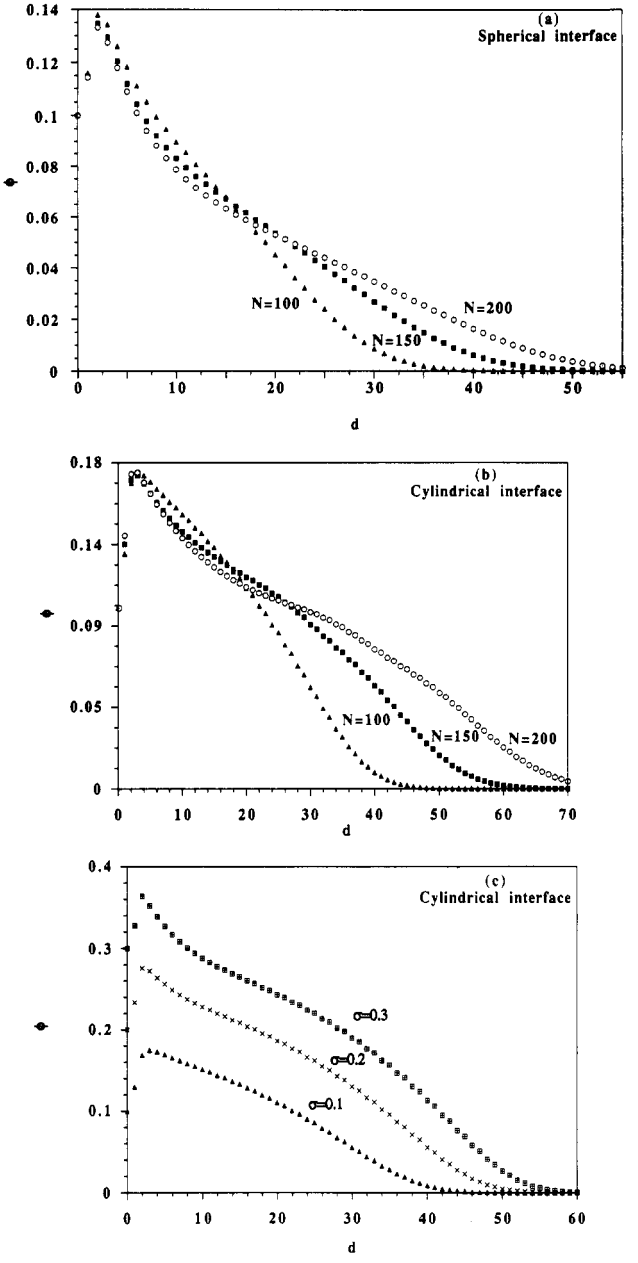

Figure 3. Effect of molecular weight and surface density on segment density distribution. $R = 10$. (a) Spherical interface, $\sigma = 0.1$. (▲) $N = 100$, (■) N = 150, (⊙) $N = 200$. (b) Cylindrical interface, $\sigma = 0.1$. (▲) $N = 100$, (■) $N = 150$, (⊙) $N = 200$. (c) Cylindrical interface, N = 100. (▲) $\sigma = 0.1$, (×) $\sigma = 0.2$, (⊞) $\sigma = 0.3$.

least-squares fit we find that the distribution of chain ends in the spherical interface case approaches the Gaussian form as the interface radius decreases (χ^2 values of the best parametric fits were 4.5×10^{-4}, 2.7×10^{-4}, and 3.9×10^{-5} for $R = 100$, 30, and 10, respectively). However, even in the low-curvature brush ($R = 100$) the end distribution is closer to the Gaussian than to the planar brush form.

As the interface curvature increases, a zone from which chain ends are excluded develops near the interface. The exclusion zone is not immediately apparent in the normalized chain end distributions, except in the high molecular weight, high curvature limit (Figure 7c). The distribution of the chain ends becomes broader and shifts away from the interface with decreasing curvature. In the cylindrical interface case, for example, the variance in the end segment distribution increases from 11 to 16 as the interface radius increases from 10 to 100. It should be noted that, in all cases examined, a large fraction of the

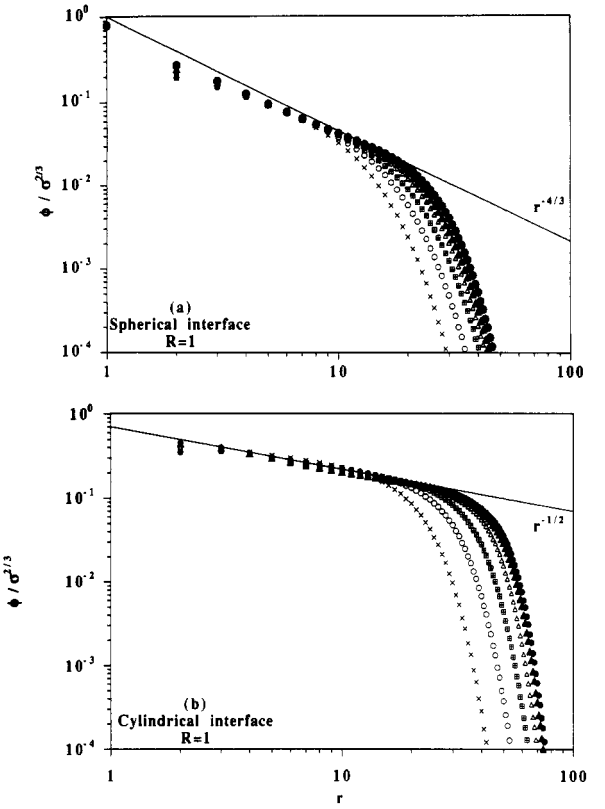

Figure 4. Segment density distribution as a function of r, normalized by $\sigma^{2/3}$. All distributions collapse after the normalization, thereby verifying the scaling $\phi \sim \sigma^{2/3}$ prediction. (a) Spherical geometry. The solid line denotes the scaling model power law (eq 1). (b) Cylindrical geometry. The solid line denotes a $-1/2$ power law. The scaling model prediction is of $-2/3$. (×) $\sigma = 0.1$, $N = 100$, (○) $\sigma = 0.1$, N = 150, (⊞) $\sigma = 0.1$, $N = 200$, (△) $\sigma = 0.2$, $N = 200$, (▲) $\sigma = 0.3$, N = 200, (●) $\sigma = 0.35$, $N = 200$.

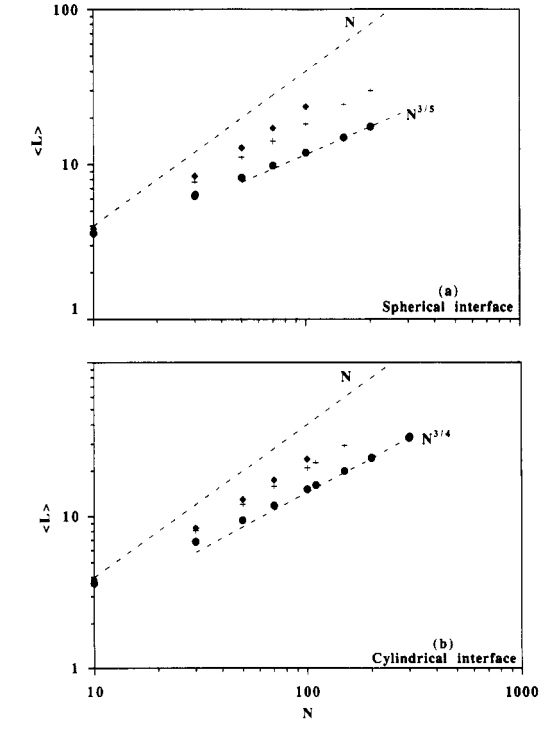

Figure 5. Brush thickness as a function of chain molecular weight. $L \sim N$ is the scaling limit for a planar brush. $\sigma = 0.1$. (a) Spherical geometry. (b) Cylindrical geometry. (◆) $R/a = 100$, (+) $R/a = 10$, (●) $R/a = 1$.

chain ends is located beyond the average brush thickness at $d/\langle L \rangle$ larger than 1. We define the thickness of the exclusion zone (x_Q) as the distance from the interface at

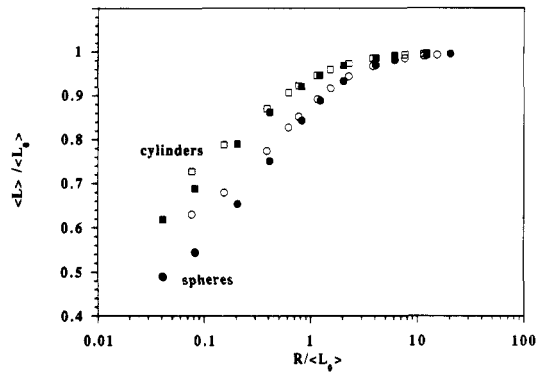

Figure 6. Brush thickness as a function of the interface radius, normalized by the planar brush thickness (L_0). $\sigma = 0.1$. Open symbols denote $N = 50$ and solid symbols $N = 100$. (○) Spherical interface. (□) Cylindrical interface.

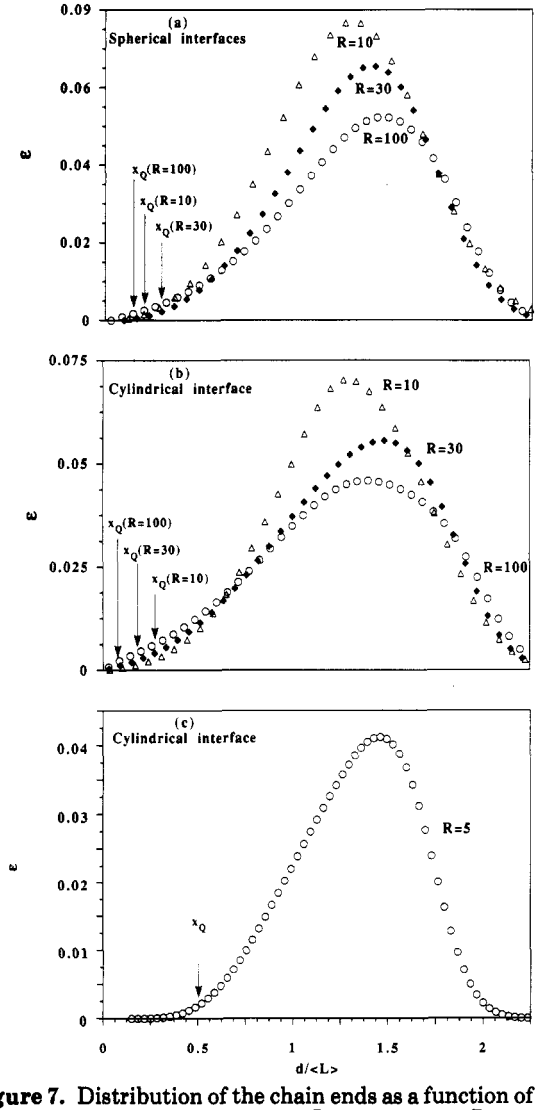

Figure 7. Distribution of the chain ends as a function of $d/\langle L\rangle$. (a) Sphere, $N = 150$, $\sigma = 0.1$. (○) $R/a = 100$, (◆) $R/a = 30$, (△) $R/a = 10$. (b) Cylinder, $N = 150$, $\sigma = 0.1$. (○) $R/a = 100$, (◆) $R/a = 30$, (△) $R/a = 10$. (c) Cylindrical geometry, $N = 300$, $R = 5$, $\sigma = 0.3$. The definition of the exclusion zone thickness, x_Q, is given in the text.

which the density of the chain ends reaches 5% of its value at the peak. For large interface radii ($R \gg \langle L\rangle$) we find, using this definition, that there is no exclusion zone ($x_Q = 0$), consistent with the planar brush analysis.[12] Alternatives to this arbitrary definition of the chain end exclusion zone give similar values of x_Q.

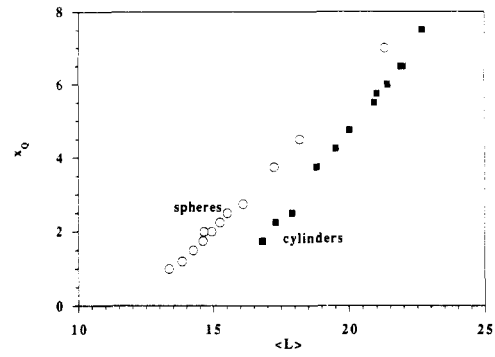

Figure 8. Chain end exclusion zone thickness as a function of the brush thickness for $N = 100$ and various surface densities and interface radii. In all cases R/L does not exceed 0.2. The slope of x_Q vs $\langle L\rangle$ is approximately 0.75 for spheres and 0.95 for cylinders. (○) Spherical interfaces. (■) Cylindrical interfaces.

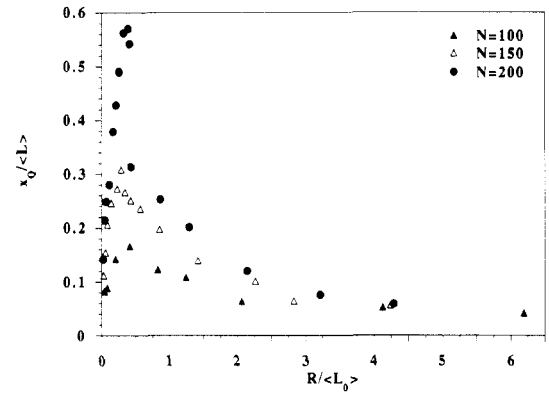

Figure 9. Normalized chain end exclusion zone as a function of the interface radius for chains on cylindrical interfaces. L_0 is the planar brush thickness. $\sigma = 0.1$. (▲) $N = 100$, (△) $N = 150$, (●) $N = 200$.

For highly curved interfaces, the exclusion zone thickness is found to vary linearly with the brush thickness, as shown in Figure 8 for both geometries. This linearity is in good agreement with analytical SCF model predictions.[5] However, the ratio of the cylindrical brush exclusion zone height to brush thickness $x_Q/\langle L\rangle$ (Figure 9) as a function of interface radius does not decrease smoothly from a maximum at $R \sim 0$ as predicted[5] but obtains a maximal value at a finite interface radius. The distribution narrows with increased molecular weight or surface densit, and the value of the maximal ratio increases. The peak position seems to be fairly insensitive to variations in system parameters.

In order to evaluate the effect of finite chain molecular weight on the exclusion zone thickness, we plot $x_Q/\langle L\rangle$ as a function of $1/N$ in Figure 10. The fluctuations in the size of the exclusion zone, relative to the brush thickness ($\Delta x_Q/\langle L\rangle$), have been shown[20] to scale as $(R_g/\langle L\rangle)^{4/3}$. In our model, the radius of gyration, R_g, is proportional to $aN^{1/2}$, and the cylindrical brush thickness, in the limit of high curvature and molecular weight, scales as $aN^{3/4}$ (see Figure 5b). The fluctuations in exclusion zone thickness should, therefore, decay as $N^{-1/3}$. We see from Figure 10 that, for the three radii examined, the extent of the exclusion zone can be fit quite well with a function of the form $A - BN^{-n}$. A three-parameter, least-squares fit yields n values between 0.2 and 0.5. A is the fraction of the brush from which chain ends are excluded, in the infinite N limit. Using a power law fit of $n = 1/3$, the value of A is largest for $R = 5$. This is consistent with the results shown in Figure 9; $R = 1$ approximately corresponds to the origin, while $R = 5$ is somewhat closer to the peak position.

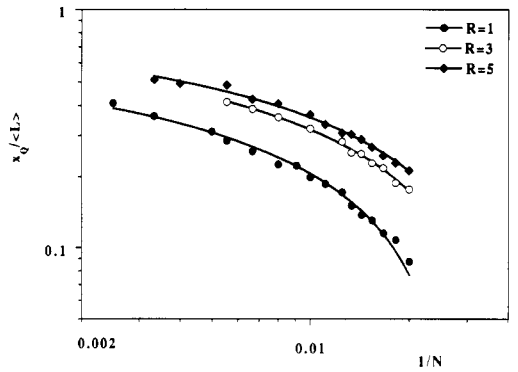

Figure 10. Normalized chain end exclusion zone as a function of the inverse molecular weight, for chains on cylindrical interfaces. $\sigma = 0.3$. A three-parameter, least-squares fit to the equation $x_Q/\langle L\rangle = A - B(1/N)^n$ gives $n = 0.21$ for $R = 1$, $n = 0.39$ for $R = 3$, and $n = 0.5$ for $R = 5$. The curve fits shown have the form of $A - B(1/N)^{1/3}$. $A(R=5) = 0.92$, $A(R=3) = 0.87$, $A(R=1) = 0.70$. (●) $R = 1$, (○) $R = 3$, (◆) $R = 5$.

Conclusions

We have examined the properties of finite chains tethered on curved interfaces using the Dolan–Edwards SCF method. We establish that significant deviations from the planar brush are seen when the interface radius is about an order of magnitude larger than the brush thickness, for both spherical and cylindrical interfaces. Therefore, as expected, accounting for interface curvature is important when the chain dimensions and the interface radius are comparable. A transition from parabolic-like profiles for low-curvature interfaces to a concave profile in the high-curvature limit is observed, as predicted by the analytical solutions of the SCF models.[5,12] In all cases the segment density profiles from SCF were in good agreement with results of MD simulation.[3,4] The density profile of chains tethered on spherical interfaces generally follows scaling model predictions in the limit of small interface radii and high chain molecular weight. However, in the case of cylindrical interfaces we do not observe the expected scaling power law of $-2/3$ for the falloff of segment density with distance. Brush thickness increased, in the limit of high curvature, as $N^{3/(3+D)}$ in both geometries.

As the interface curvature increases, a zone from which chain ends are excluded develops near the interface, and the distribution of chain end position becomes narrower. The exclusion zone height increases linearly with brush thickness in layers where the brush thickness was much larger than interface radius in both geometries. Although our calculations apply to systems of chains in a good solvent, these results are in good agreement with the predictions of Ball et al.[5] for chains in the melt on cylindrical interfaces. However, we do not find that, in the cylindrical brush, the ratio of exclusion zone height to layer thickness obtains a maximum value at infinite interface curvature ($R \sim 0$). Rather, the maximum ratio occurs at a finite interface radius of approximately 0.35-$\langle L_0\rangle$ and seems to be invariant to either chain molecular weight or surface density. It is curious to note that the peak position is fairly constant, but the fraction of the brush from which chain ends are excluded increases with molecular weight. The corrections to the infinite molecular weight limit, for the fraction of the brush from which chain ends are excluded, can be fit reasonably well by the predicted[19] scaling form of $N^{-1/3}$.

We can conclude that interface curvature is important in determining tethered chain behavior when the interface radius is within an order of magnitude of the chain dimensions. In such cases, we confirm here that scaling models provide a fairly good estimate of the brush thickness. However, scaling models do not probe the internal brush structure, which is important in determining the distribution of chain ends and in evaluating the interactions between layers. The presence of an exclusion zone in the chain end distribution is significant since it can be manipulated to exclude chain ends from the region near the interface, thereby localizing the ends at the outer edge of the layer and modifying the layer surface. The interaction range of a finite molecular weight brush is far larger than the average brush thickness. Chain ends extending beyond the average brush height pay a comparatively low energetic penalty, so that a "tail" is formed in the segment density distribution.[16,19] The tail region is not accounted for in analytical SCF models[5,12] because, for an infinite chain, the energy cost for chain ends extending beyond the average brush height is prohibitive. The size of the segment density tail, which is also observed in the planar brush,[13,19] is especially significant in highly curved interfaces where the density profile decays more rapidly. Tails can be expected to play an important role in the rheology of systems of polymer brushes grafted to small particles, since tails largely determined the hydrodynamic layer thickness for layers immersed in solvent[17] and are the potential participants in interlayer entanglements in dense suspensions.[16]

Acknowledgement is made to the donors of the Petroleum Research Fund, administered by the American Chemical Society, for partial support of this research. Partial support was also received, with appreciation, from the National Science Foundation (NSF/CTS-9107025, Interfacial Transport and Separations Program [CTS] and Polymers Program [DMR]). This research was partially supported by a grant of computer time from the Minnesota Supercomputer Institute. We thank S. T. Milner, T. A. Witten, and especially J. F. Marko for helpful discussions.

References and Notes

(1) Halperin, A.; Tirrell, M.; Lodge, T. P. *Adv. Polym. Sci.* **1992**, *100*, 31.
(2) Milner, S. T. *Science* **1991**, *252*, 905.
(3) Grest, G. S.; Kremer, K.; Witten, T. A. *Macromolecules* **1987**, *20*, 1376.
(4) Murat, M.; Grest, G. S. *Macromolecules* **1991**, *24*, 704.
(5) Ball, R. C.; Marko, J. F.; Milner, S. T.; Witten, T. A. *Macromolecules* **1991**, *24*, 693.
(6) Daoud, M.; Cotton, J. P. *J. Phys. (Paris)* **1982**, *43*, 531.
(7) Birshtein, T. M.; Zhulina, E. B.; Khokhlov, A. R.; Yurasova, T. A. *Polym. Sci. USSR* **1987**, *29*, 1293.
(8) Alexander, S. *J. Phys. (Paris)* **1976**, *38*, 977.
(9) de Gennes, P. G. *Scaling Concepts in Polymer Physics*; Cornell University Press: Ithaca, NY, 1979.
(10) Dolan, A. K.; Edwards, S. F. *Proc. R. Soc. London* **1975**, *A343*, 427.
(11) Semenov, A. N. *Sov. Phys. JETP* **1985**, *61*, 733.
(12) Milner, S. T.; Witten, T. A.; Cates, M. *Macromolecules* **1988**, *21*, 2610.
(13) Patel, S. S. Presented at Tethered Chains I: A Symposium on the Science of Polymeric Surfactants, Minneapolis, MN, May 1991.
(14) Khasat, N.; Pennisi, R.; Hadjichristidis, N.; Fetters, L. J. *Macromolecules* **1988**, *21*, 1100.
(15) Tsukahara, Y.; Mizuno, K.; Segawa, A.; Yamashita, Y. *Macromolecules* **1989**, *22*, 1546.
(16) Witten, T. A.; Leibler, L.; Pincus, P. A. *Macromolecules* **1990**, *23*, 824.
(17) Fredrickson, G. H.; Pincus, P. A. *Langmuir* **1991**, *7* (4), 786.
(18) Grest, G. S.; Kremer, K.; Milner, S. T.; Witten, T. A. *Macromolecules* **1989**, *22*, 1904.
(19) Milner, S. T. *J. Chem. Soc., Faraday Trans.* **1990**, *86*, 1349.
(20) Marko, J. F.; Milner, S. T., private communication.